Kobe University Repository : Kernel

PDF issue: 2025-12-05

A vertebrobasilar junction aneurysm successfully treated with a combination of surgical clipping and flow diverter placement based on the results of computational fluid…

Mori, Tatsuya ; Kimura, Hidehito ; Fujita, Atsushi ; Hayashi, Kosuke ; Hori, Tatsuo ; Sugihara, Masahiro ; Ikeuchi, Yusuke ; Kohta, Masaaki ;…

(Citation)
Journal of Neurosurgery: Case Lessons,7(10):CASE23736

(Issue Date)
2024-03-04

(Resource Type)
journal article

(Version)
Version of Record

(Rights)
© 2024 The authors
Creative Commons Attribution-NonCommercial-NoDerivatives 4.0 International license.

(URL)
https://hdl.handle.net/20.500.14094/0100488775

KOBE UNIVERSITY

JOURNAL OF NEUROSURGERY:
Case Lessons

J Neurosurg Case Lessons 7(10): CASE23736, 2024
DOI: 10.3171/CASE23736

A vertebrobasilar junction aneurysm successfully treated with a combination of surgical clipping and flow diverter placement based on the results of computational fluid dynamics analysis: illustrative case

Tatsuya Mori, MD,[1] Hidehito Kimura, MD, PhD,[1] Atsushi Fujita, MD, PhD,[1] Kosuke Hayashi, DEng,[2] Tatsuo Hori, MD, PhD,[1] Masahiro Sugihara, MD,[1] Yusuke Ikeuchi, MD,[1] Masaaki Kohta, MD, PhD,[1] Akio Tomiyama, DEng,[2] and Takashi Sasayama, MD, PhD[1]

[1]Department of Neurosurgery, Kobe University Graduate School of Medicine, Kobe, Japan; and [2]Graduate School of Engineering, Kobe University, Kobe, Japan

BACKGROUND The treatment of vertebrobasilar junction (VBJ) aneurysms is challenging. Although flow diverters (FDs) are a possible treatment option, geometrical conditions hinder intervention. VBJ aneurysms possess dual inflow vessels from the bilateral vertebral arteries (VAs), one of which is ideally occluded prior to FD treatment. However, it remains unclear which VA should be occluded.

OBSERVATIONS A 75-year-old male with a growing VBJ complex aneurysm exhibiting invagination toward the brainstem and causing perifocal edema required intervention. Preoperative computational fluid dynamics (CFD) analysis demonstrated that left VA occlusion would result in more stagnant flow and less impingement of flow than right VA occlusion. According to the simulated strategy, surgical clipping of the left VA just proximal to the aneurysm was performed, followed by FD placement from the basilar artery trunk to the right VA. The patient demonstrated tolerance of the VA occlusion, and follow-up computed tomography angiography at 18 months after FD treatment confirmed the disappearance of the aneurysm.

LESSONS Preoperative flow dynamics simulations using CFD analysis can reveal an optimal treatment strategy involving a hybrid surgery that combines FD placement and direct surgical occlusion for a VBJ complex aneurysm.

https://thejns.org/doi/abs/10.3171/CASE23736

KEYWORDS computational fluid dynamics; vertebrobasilar junction aneurysm; flow diverter; nonsaccular; wall shear stress; oscillatory shear index

Nonsaccular aneurysms of the posterior fossa are uncommon and often have a severe natural course.[1,2] Furthermore, the lack of established standard treatments renders its management challenging.[3] Recently, flow diverters (FDs) have shown promise in treating these conditions, offering occlusion rates of up to 70%. However, high perioperative complication and mortality rates are concerning.[4–7] Additionally, complex cases can require a combination of FDs with direct surgery and other endovascular methods.[8–10] Techniques involve altering the blood flow by occluding vessels before stent placement to transform the aneurysm into a sidewall type, thereby improving occlusion rates. However, few studies have simulated hemodynamic changes in such treatments.[11,12]

In this report, we present the case of a vertebrobasilar junction (VBJ) complex aneurysm the treatment of which with FDs alone was deemed challenging. On the basis of results of a computational fluid dynamics (CFD) analysis, we simulated a rational treatment strategy. Given the results of this simulation, the patient underwent direct surgery to occlude the inflow vessels followed by FD placement, resulting in a favorable outcome.

Illustrative Case

A 75-year-old male presented with a medical history of hypertension, dyslipidemia, postpercutaneous coronary intervention, and valvular heart disease. The patient was a nonsmoker with no family history of subarachnoid hemorrhage. A small aneurysm at the VBJ

ABBREVIATIONS ASA = anterior spinal artery; CFD = computational fluid dynamics; CT = computed tomography; CTA = computed tomography angiography; FD = flow diverter; IR = inflow rate; mAIRC = and modified aneurysm inflow rate coefficient; MRI = magnetic resonance imaging; OKM = O'Kelly-Marotta; OSI = oscillatory shear index; VA = vertebral artery; VBJ = vertebrobasilar junction; WSS = wall shear stress; WSSDV = wall shear stress vector direction variation.

INCLUDE WHEN CITING Published March 4, 2024; DOI: 10.3171/CASE23736.
SUBMITTED December 15, 2023. **ACCEPTED** January 29, 2024.
© 2024 The authors, CC BY-NC-ND 4.0 (http://creativecommons.org/licenses/by-nc-nd/4.0/)

Brought to you by Kobe University | Unauthenticated | Downloaded 04/24/24 01:14 AM UTC

had been incidentally found on brain magnetic resonance imaging (MRI) 6 years earlier. Initially managed with observation, the aneurysm gradually enlarged. This growth resulted in invagination toward the left pons and perifocal edema, leading to referral to our facility (Fig. 1A and B). The patient showed no neurological symptoms. Cerebral angiography revealed that the aneurysm had enlarged and bulged in a formation that included the VBJ, with its size measuring 9.61 mm to 10.84 mm, and that the vascular architecture on the ventral side of the aneurysm was preserved (Fig. 1C–F). The anterior spinal artery (ASA) originated from a nonlesion part of the left vertebral artery (VA; Fig. 1E).

Considerations

Treating a complex-shaped aneurysm with simple clipping or stent-assisted coil embolization is challenging.[2] Therefore, we decided to adopt a treatment strategy involving occlusion of the unilateral VA followed by FD placement. To determine the optimal side for VA occlusion, CFD analysis was conducted using the commercial software hemoscope (EBM Corp.), based on computed tomography angiography (CTA) data. The CFD analysis method is similar to that described in a previous study.[13] Simulations of hemodynamic changes within the aneurysm were performed for each occlusion strategy of the right or left VA. When the right VA was occluded, blood flow from the left VA created an impingement flow against the aneurysm wall, resulting in increased wall shear stress (WSS) at the collision site and reduced wall shear stress vector direction variation (WSSDV) and oscillatory shear index (OSI; Fig. 2A–D). In contrast, occlusion of the left VA resulted in blood flow from the right VA, spiraling through the aneurysm toward the basilar artery. This pattern suggested a stagnant flow within the aneurysm, as evidenced by the observed increases in the WSSDV and OSI (Fig. 2E–H). The latter hemodynamic condition was considered preferable for successful aneurysm occlusion after FD treatment.

Treatment

A balloon occlusion test was conducted to confirm tolerance of the occlusion of the left VA. The initial surgery was attempted using an anterior petrosal approach to occlude the left VA. However, the segment of the left VA just proximal to the aneurysm was not visualized, and the occlusion was abandoned. Two months after the initial surgery, a retrosigmoid approach via a left suboccipital craniotomy was performed (Fig. 3A and B), successfully achieving left VA occlusion. Surgery was performed with the patient in the park-bench position. Appropriate cerebrospinal fluid drainage and release of the horizontal fissure facilitated access to the ventral surface of

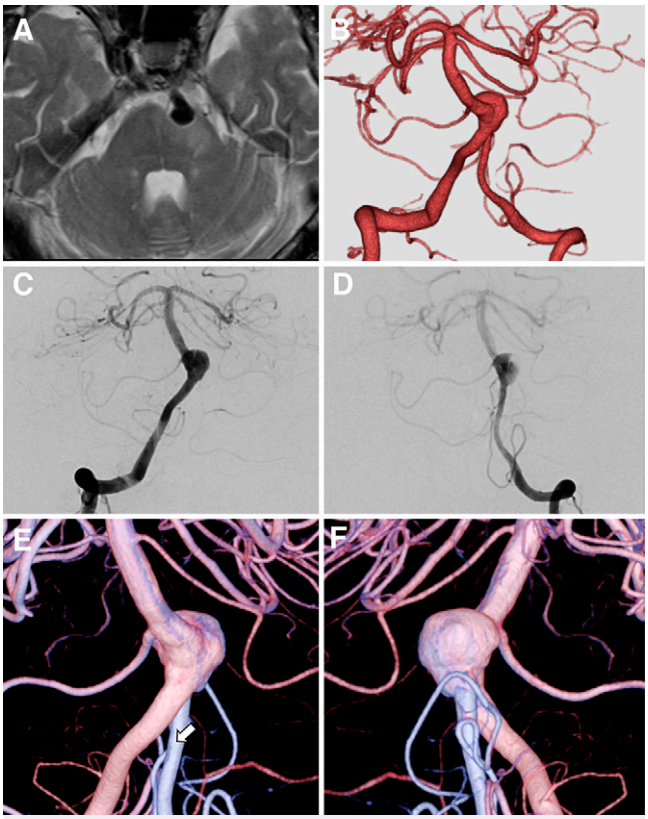

FIG. 1. Axial T2-weighted MRI (**A**) showing an aneurysm embedded in the brainstem with perifocal edema. The VBJ complex aneurysm was identified using CTA (**B**). Anteroposterior right (**C**) and left (**D**) VA digital subtraction angiography (DSA). Anteroposterior (**E**) and posteroanterior (**F**) three-dimensional rotational angiography fusion images. *Arrows* indicate branching of the ASA.

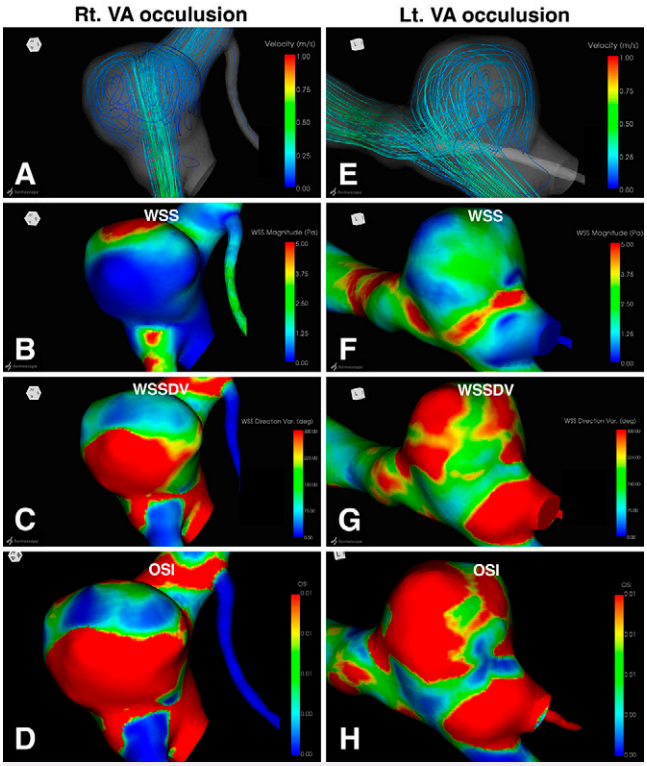

FIG. 2. Preoperative CFD analysis. **A:** The streamline patterns demonstrate impingement of blood flow. **B:** Elevated values of WSS are observed in the impingement area. **C:** Lower values of WSSDV are present in the impingement area. **D:** Lower values of OSI are observed in the impingement area. **E:** The streamline patterns indicate the presence of swirling blood flow. **F:** The distribution of WSS is relatively uniform, exhibiting low values. **G:** The distribution of WSSDV is relatively uniform with high values. **H:** The distribution of OSI is relatively uniform, exhibiting high values.

Brought to you by Kobe University | Unauthenticated | Downloaded 04/24/24 01:14 AM UTC

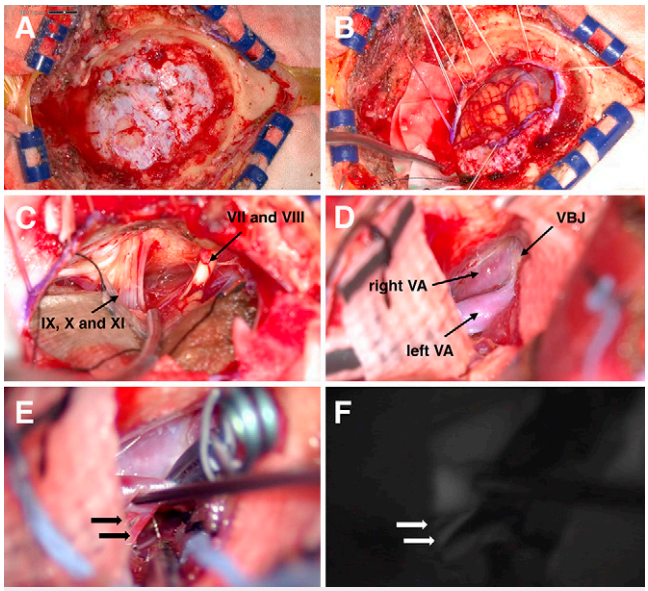

FIG. 3. A: A retrosigmoid approach was performed via a left suboccipital craniotomy. The craniotomy was extended enough to expose the transverse sinus and sigmoid sinus. The inferior extent of the craniotomy did not reach the condylar fossa. **B:** Cerebrospinal fluid was evacuated from the lateral cerebellomedullary cistern, and the dura was incised along the sinus. **C:** The lower cranial nerves and cranial nerves VII and VIII were identified, and the horizontal fissure was released to improve visualization toward the brainstem. **D:** The dorsal aspect of the left VA was visualized. **E:** Two perforators emanating from the posterior aspect of the left VA were identified, and the left VA was occluded just distal to these perforators (*black arrows*). **F:** Preservation of the two perforators (*white arrows*) was confirmed using indocyanine green angiography.

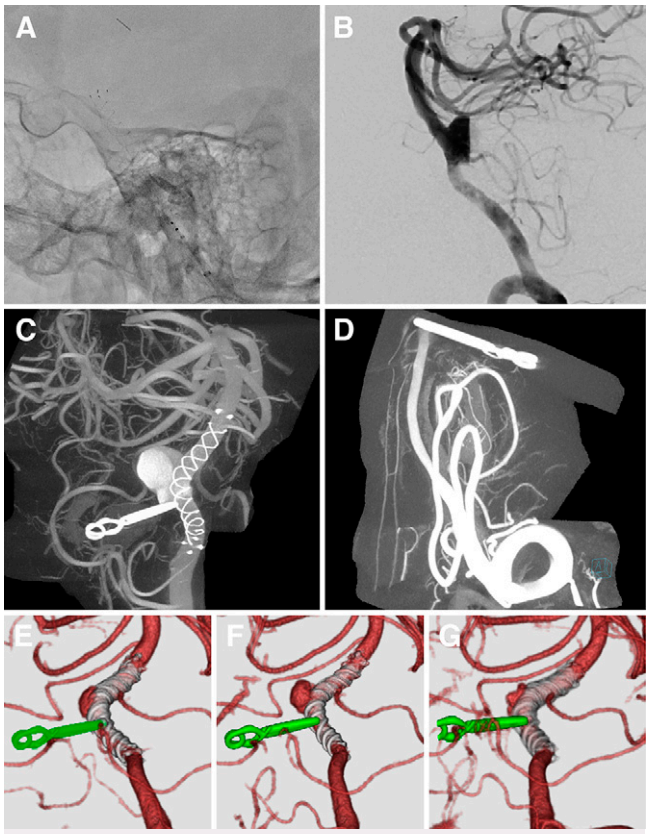

FIG. 4. A: Postplacement lateral fluoroscopy images of the FD. **B:** Lateral DSA indicates that blood is stagnant within the aneurysm fundus. **C:** Cone beam CT confirms appropriate placement of the FD. **D:** Cone beam CT demonstrates preservation of the ASA proximal to the clip. **E:** CTA at 6 months post-FD placement shows obliteration at OKM grade C. **F:** CTA at 12 months post-FD placement reveals a worsened occlusion status at OKM grade B. **G:** CTA at 18 months post-FD placement indicates an improvement in occlusion status to OKM grade C.

the brainstem (Fig. 3C and D). Two perforators were identified in the posterior aspect of the left VA. Occlusion was performed immediately distal to these perforators using a Sugita clip (Mizuho Medical; Fig. 3E and F).

Dual antiplatelet therapy was initiated 1 week after the second surgery. Two weeks later, the FD placement procedure was performed. Initially, a 5-Fr SOFIA SELECT catheter (MicroVention/Terumo) was guided to the intracranial segment of the right VA, followed by advancing a Headway 27 microcatheter (MicroVention/Terumo) to the distal end of the basilar artery. A FRED 4.0 × 32 mm (MicroVention/Terumo) stent was then deployed, starting from the midbasilar artery and positioned along the curvature of the right VA (Fig. 4A and B). Cone-beam computed tomography (CT) confirmed adequate wall apposition of the stent and preservation of the perforators and ASA (Fig. 4C and D). This negated the need for additional percutaneous transluminal angioplasty. Furthermore, coil embolization within the aneurysm was not performed considering its potential impact on brainstem compression.

Outcome and Follow-Up

The patient exhibited no significant complications in the postoperative course and was discharged with residual left facial numbness, a sequela of the initial surgery, corresponding to a modified Rankin Scale score of 1. Six months after FD treatment, angiographic examination revealed an occlusion status of O'Kelly-Marotta (OKM) grade C (Fig. 4E). MRI still did not show resolution of the perifocal brain edema. At this time, the antiplatelet therapy was adjusted to aspirin monotherapy. Seven months after FD treatment, the patient underwent cardiac surgery for mitral valve insufficiency and pacemaker implantation for sick sinus syndrome, with edoxaban added to the regimen. At 12 months after FD treatment, worsening of the occlusion status of the aneurysm to OKM grade B was observed (Fig. 4F). Consequently, the antithrombotic treatment was modified to edoxaban monotherapy and aspirin was discontinued. At 18 months after FD treatment, CTA showed improvement in the occlusion status of the aneurysm to OKM grade C (Fig. 4G).

Patient Informed Consent

The necessary patient informed consent was obtained in this study.

Discussion

Observations

For the treatment of VBJ aneurysms, the strategy of occluding one side of the VA, modifying the aneurysm into a sidewall type,

Brought to you by Kobe University | Unauthenticated | Downloaded 04/24/24 01:14 AM UTC

and then placing an FD stent demonstrated effectiveness. The introduction of CFD analysis to determine the best occlusion side led to nearly complete occlusion of the aneurysm.

In the treatment of posterior circulation aneurysms using FD devices, a 1-year postoperative occlusion rate of 66% to 78% is observed, with morbidity and mortality rates of 11% to 27%.[4–6] Additionally, when focusing on nonsaccular aneurysms, treatment challenges are highlighted by a lower occlusion rate of 52% and a substantial combined morbidity and mortality rate of 47%.[7] The presence of side branches has been identified as a predictive factor for occlusion after FD treatment.[14–17] Consequently, strategies involving the occlusion of inflow or outflow vessels prior to FD placement have been reported; however, in cases in which the VA was sacrificed using coils, brainstem infarctions occurred in two of six cases.[18–20] In our case, surgical trapping was performed to occlude the left VA while visually confirming a small perforator arising from the left VA and finally preserving it, resulting in no complications and a favorable outcome. In the surgical trapping of the VA, direct surgery is more ideal than endovascular internal trapping for placing clips while observing nearby branching arteries and thus reducing postoperative infarction risks despite the risk of cranial nerve palsy.[21] Endovascular internal trapping is effective but carries a high risk of perforator infarction.[22] In this case, occlusion just proximal to the VA union in a short segment was required; therefore, endovascular treatment was considered particularly challenging.

In our case study, favorable occlusion was achieved using CFD analysis to determine the optimal occlusion site. When simulating blood flow after occluding the right VA, we observed that blood flow directed toward the aneurysm was altered as an impingement flow, creating a point of high WSS on the aneurysm wall. This flow pattern was considered to potentially lead to aneurysm enlargement, bleb formation, or rupture because of the high divergence of the WSS, which promoted stretching of the aneurysm wall.[23–25] In cases in which a strong inflow jet remains after FD placement, occlusion of the aneurysm are difficult to achieve.[26] Conversely, occlusion of the left VA resulted in blood flow swirling toward the aneurysm and exiting the basilar artery. This led to increased WSSDV and OSI, which are indicators of blood flow stagnation within the aneurysm.[13,27] Given that a higher degree of stagnation is thought to accelerate thrombosis within the aneurysm post-FD treatment, the decision to occlude the left VA was made (Fig. 2).

In CFD studies for predicting occlusion after FD deployment, parameters such as flow velocity, WSS, shear rate, aneurysm inflow rate (IR), and modified aneurysm inflow rate coefficient (mAIRC) have been reported as useful indicators.[26,28,29] The parameters measured using the hemoscope are presented in Table 1. A reduction in hemodynamics, particularly in terms of WSS and IR, is a crucial mechanism that induces intraaneurysmal thrombosis.[28] In vitro flow-induced thrombosis was seen to occur at a specific WSS threshold of 0.41 Pa.[30] Additionally, studies have demonstrated that in terms of the hemodynamics prior to FD placement, a lower WSS and IR value are associated with a higher occlusion rate.[26,28,29] Therefore, in this case, the lower mean WSS and IR at the right VA occlusion than at the left VA occlusion suggested a preferential strategy for right VA occlusion. However, the left VA was hypoplastic compared to the right VA, indicating a potential increase in these values due to the remodeling associated with contralateral occlusion. Therefore, these observations did not influence the decision about the side of occlusion in this particular case. The mAIRC denotes the proportion of the aneurysmal inflow rate to the flow rate in the proximal parent artery. No significant differences were observed in mAIRC. Previously, we reported that aneurysms with greater variations in WSS during a cardiac cycle are at a higher risk for enlargement, supporting the decision for left VA occlusion.[31]

TABLE 1. Comparison of hemodynamic parameters

Variable	Lt VA Occlusion	Rt VA Occlusion
Mean WSS in Pa	2.189	1.571
WSS, systolic phase in Pa	3.863	4.991
WSS, diastolic phase in Pa	1.836	1.683
Flow rate of preserved VA in mL/min	190.6	101.0
Aneurysm inflow rate in mL/min	212.1	96.54
mAIRC	1.11	0.956
Diameter of preserved VA in mm	4.45	3.58

In the postoperative course of this case, there was transient worsening of the occlusive state, likely due to the antithrombotic medication. A study has shown that among patients treated with FD treatment and concomitant anticoagulation therapy, six of eight did not attain complete occlusion.[32] Therefore, caution should be exercised in patients with conditions that require anticoagulation therapy.

Technical limitations prevented the simulation of blood flow conditions after stent deployment. Utilizing CFD analysis with porous media could enable a comparison of pre- and poststent placement conditions, thereby allowing for a more comprehensive assessment.[28,33] Moreover, this treatment strategy may not eliminate the risk of perforator occlusion. In this case, clipping rather than coiling could occlude the VA over a shorter segment while ensuring that the perforating branches are preserved. However, caution is required, because blind ending of the vessels can result in delayed occlusion of the perforators.[34,35]

Lessons

Simulating flow dynamics before surgery using CFD analysis can help to identify a more effective treatment involving a hybrid surgical technique that integrates FD placement and direct surgical occlusion of a VBJ complex aneurysm. In CFD analysis to determine the optimal occlusion side, examining the stagnation of blood flow within the aneurysm is useful.

References

1. Bhogal P, Pérez MA, Ganslandt O, Bäzner H, Henkes H, Fischer S. Treatment of posterior circulation non-saccular aneurysms with flow diverters: a single-center experience and review of 56 patients. *J Neurointerv Surg.* 2017;9(5):471–481.
2. Wakhloo AK, Mandell J, Gounis MJ, et al. Stent-assisted reconstructive endovascular repair of cranial fusiform atherosclerotic and dissecting aneurysms: long-term clinical and angiographic follow-up. *Stroke.* 2008;39(12):3288–3296.
3. Algra AM, Lindgren A, Vergouwen MDI, et al. Procedural clinical complications, case-fatality risks, and risk factors in endovascular and neurosurgical treatment of unruptured intracranial aneurysms: a systematic review and meta-analysis. *JAMA Neurol.* 2019;76(3):282–293.
4. Taschner CA, Vedantham S, de Vries J, et al. Surpass flow diverter for treatment of posterior circulation aneurysms. *AJNR Am J Neuroradiol.* 2017;38(3):582–589.

Brought to you by Kobe University | Unauthenticated | Downloaded 04/24/24 01:14 AM UTC

5. Bender MT, Colby GP, Jiang B, et al. Flow diversion of posterior circulation cerebral aneurysms: a single-institution series of 59 cases. *Neurosurgery.* 2019;84(1):206–216.
6. Griessenauer CJ, Ogilvy CS, Adeeb N, et al. Pipeline embolization of posterior circulation aneurysms: a multicenter study of 131 aneurysms. *J Neurosurg.* 2018;130(3):923–935.
7. Kiyofuji S, Graffeo CS, Perry A, et al. Meta-analysis of treatment outcomes of posterior circulation non-saccular aneurysms by flow diverters. *J Neurointerv Surg.* 2018;10(5):493–499.
8. Sato K, Endo H, Fujimura M, et al. Endovascular treatments in combination with extracranial-intracranial bypass for complex intracranial aneurysms. *World Neurosurg.* 2018;113:e747–e760.
9. Oishi H, Teranishi K, Yatomi K, Fujii T, Yamamoto M, Arai H. Flow diverter therapy of a giant fusiform vertebrobasilar junction aneurysm in a child: case report. *NMC Case Rep J.* 2018;6(1):25–28.
10. Kalani MYS, Zabramski JM, Nakaji P, Spetzler RF. Bypass and flow reduction for complex basilar and vertebrobasilar junction aneurysms. *Neurosurgery.* 2013;72(5):763–776.
11. Hassan T, Ezura M, Timofeev EV, et al. Computational simulation of therapeutic parent artery occlusion to treat giant vertebrobasilar aneurysm. *AJNR Am J Neuroradiol.* 2004;25(1):63–68.
12. Walcott BP, Reinshagen C, Stapleton CJ, et al. Predictive modeling and in vivo assessment of cerebral blood flow in the management of complex cerebral aneurysms. *J Cereb Blood Flow Metab.* 2016;36(6):998–1003.
13. Kimura H, Taniguchi M, Hayashi K, et al. Clear detection of thin-walled regions in unruptured cerebral aneurysms by using computational fluid dynamics. *World Neurosurg.* 2019;121:e287–e295.
14. Burkhardt JK, Tanweer O, Nelson PK, Riina HA. Editorial. Indication and technique for using the Pipeline embolization device to treat intracranial aneurysms. *J Neurosurg.* 2018;130(1):256–258.
15. Hanel RA, Monteiro A, Nelson PK, Lopes DK, Kallmes DF. Predictors of incomplete aneurysm occlusion after treatment with the Pipeline Embolization Device: PREMIER trial 1 year analysis. *J Neurointerv Surg.* 2022;14(10):1014–1017.
16. Park MS, Mazur MD, Moon K, et al. An outcomes-based grading scale for the evaluation of cerebral aneurysms treated with flow diversion. *J Neurointerv Surg.* 2017;9(11):1060–1063.
17. Meyer L, Stracke CP, Bester M, et al. Predictors of aneurysm occlusion after treatment with flow diverters: a systematic literature review. *J Neurointerv Surg.* Published online June 14, 2023. doi: jnis-2022-019993.
18. Hosoo H, Tsuruta W, Dofuku S, Hara T, Ishikawa E, Matsumaru Y. Delayed occlusion of the anterior choroidal artery following flow diverter stent deployment for unruptured aneurysm: a case report and literature review. *NMC Case Rep J.* 2021;8(1):167–175.
19. Siddiqui AH, Abla AA, Kan P, et al. Panacea or problem: flow diverters in the treatment of symptomatic large or giant fusiform vertebrobasilar aneurysms. *J Neurosurg.* 2012;116(6):1258–1266.
20. Natarajan SK, Lin N, Sonig A, et al. The safety of Pipeline flow diversion in fusiform vertebrobasilar aneurysms: a consecutive case series with longer-term follow-up from a single US center. *J Neurosurg.* 2016;125(1):111–119.
21. Tsunoda S, Inoue T. Microsurgical treatment strategy of vertebral artery fusiform aneurysm-from the standpoint of hemodynamic integrity and perforator preservation. *Front Neurol.* 2021;12:728176.
22. Endo H, Matsumoto Y, Kondo R, et al. Medullary infarction as a poor prognostic factor after internal coil trapping of a ruptured vertebral artery dissection. *J Neurosurg.* 2013;118(1):131–139.
23. Kim JH, Han H, Moon YJ, et al. Hemodynamic features of microsurgically identified, thin-walled regions of unruptured middle cerebral artery aneurysms characterized using computational fluid dynamics. *Neurosurgery.* 2020;86(6):851–859.
24. Meng H, Tutino VM, Xiang J, Siddiqui A. High WSS or low WSS? Complex interactions of hemodynamics with intracranial aneurysm initiation, growth, and rupture: toward a unifying hypothesis. *AJNR Am J Neuroradiol.* 2014;35(7):1254–1262.
25. Frösen J, Cebral J, Robertson AM, Aoki T. Flow-induced, inflammation-mediated arterial wall remodeling in the formation and progression of intracranial aneurysms. *Neurosurg Focus.* 2019;47(1):E21.
26. Mut F, Raschi M, Scrivano E, et al. Association between hemodynamic conditions and occlusion times after flow diversion in cerebral aneurysms. *J Neurointerv Surg.* 2015;7(4):286–290.
27. Kimura H, Osaki S, Hayashi K, et al. Newly identified hemodynamic parameter to predict thin-walled regions of unruptured cerebral aneurysms using computational fluid dynamics analysis. *World Neurosurg.* 2021;152:e377–e386.
28. Beppu M, Tsuji M, Ishida F, Shirakawa M, Suzuki H, Yoshimura S. Computational fluid dynamics using a porous media setting predicts outcome after flow-diverter treatment. *AJNR Am J Neuroradiol.* 2020;41(11):2107–2113.
29. Paliwal N, Jaiswal P, Tutino VM, et al. Outcome prediction of intracranial aneurysm treatment by flow diverters using machine learning. *Neurosurg Focus.* 2018;45(5):E7.
30. Corbett SC, Ajdari A, Coskun AU, N-Hashemi H. In vitro and computational thrombosis on artificial surfaces with shear stress. *Artif Organs.* 2010;34(7):561–569.
31. Kimura H, Hayashi K, Taniguchi M, et al. Detection of hemodynamic characteristics before growth in growing cerebral aneurysms by analyzing time-of-flight magnetic resonance angiography images alone: preliminary results. *World Neurosurg.* 2019;122:e1439–e1448.
32. Fujii T, Oishi H, Teranishi K, Yatomi K, Suzuki K, Arai H. Outcome of flow diverter placement for intracranial aneurysm with dual antiplatelet therapy and oral anticoagulant therapy. *Interv Neuroradiol.* 2020;26(5):532–538.
33. Chong W, Zhang Y, Qian Y, Lai L, Parker G, Mitchell K. Computational hemodynamics analysis of intracranial aneurysms treated with flow diverters: correlation with clinical outcomes. *AJNR Am J Neuroradiol.* 2014;35(1):136–142.
34. Endo H, Sato K, Kondo R, Matsumoto Y, Takahashi A, Tominaga T. Tuberothalamic artery infarctions following coil embolization of ruptured posterior communicating artery aneurysms with posterior communicating artery sacrifice. *AJNR Am J Neuroradiol.* 2012;33(3):500–506.
35. Ravina K, Strickland BA, Rennert RC, et al. Fusiform vertebral artery aneurysms involving the posterior inferior cerebellar artery origin associated with the sole angiographic anterior spinal artery origin: technical case report and treatment paradigm proposal. *J Neurosurg.* 2018;131(4):1–7.

Disclosures

The authors report no conflict of interest concerning the materials or methods used in this study or the findings specified in this paper.

Author Contributions

Conception and design: Kimura, Mori, Fujita, Tomiyama. Acquisition of data: Kimura, Mori, Fujita, Hori, Ikeuchi, Kohta. Analysis and interpretation of data: Kimura, Mori, Fujita, Hayashi, Hori. Drafting the article: Kimura, Mori, Fujita, Hayashi, Hori. Critically revising the article: Fujita, Hayashi, Kohta. Reviewed submitted version of manuscript: Fujita, Hayashi, Sugihara, Kohta. Approved the final version of the manuscript on behalf of all authors: Kimura. Administrative/technical/material support: Fujita. Study supervision: Sasayama.

Correspondence

Hidehito Kimura: Kobe University Graduate School of Medicine, Chuo-ku, Kobe, Japan. hkimura@med.kobe-u.ac.jp.

Brought to you by Kobe University | Unauthenticated | Downloaded 04/24/24 01:14 AM UTC